DETECTION AND REMOVAL OF RAINBOW EFFECT ARTIFACTS

Lanlan Chang, Yap-Peng Tan, and Hock-Chuan Chua

School of Electrical and Electronic Engineering
Nanyang Technological University
50 Nanyang Avenue, 639798, Singapore

ABSTRACT

Due to the imperfect separation of luminance and chroma signals in receiver's demodulation, composite video signals suffer from rainbow effect artifacts, which present themselves as interlaced color stripes in regions of high luminance frequency and high luminance intensity. In this paper, we derive the formulas governing the rainbow effects. Based on these formulas, we propose a novel method to detect and remove these annoying artifacts. Experimental results on both captured video frames and simulated frames show that our method can remove the rainbow-effect artifacts effectively and improve the image quality notably.

Index Terms—Rainbow Effect, Chroma Noise, Artifact Detection, Artifact Removal, Composite Video.

1. INTRODUCTION

Composite video signals suffer from rainbow effects, a kind of chroma noise, due to the imperfect separation of luminance and chroma components in decoding the video signals by the receivers [1, 2]. Rainbow effect artifacts present themselves as interlaced color stripes, usually in purple-green or orange-blue, and appear in regions of high luminance frequency and high luminance intensity as illustrated in Figure 1 (covering the surface of the tennis racket). These artifacts are annoying, showing up as rolling color stripes in motion pictures.

Fig. 1. Example of rainbow effect artifacts.

The cause of rainbow effect is stated in [1, 2]. An AviSynth plugin called GuavaComb filter was proposed for removing the artifacts during post-processing of captured videos [2]. This filter exploits the temporal correlation of chroma and simply averages the chrominance components of two neighboring frames. Another proposal for removing rainbow effect is using a VirtualDub plugin called Smart Smoother IQ filter (SMIQ) [3]. SMIQ filter applies spatial filtering in chrominance components to remove the abrupt changes. Some results of using these two filters can be found in Section 5. We observe residue artifacts in the restoration results using GuavaComb filter as well as by SMIQ filter. Furthermore, we observe that applying a spatial or temporal filter to the entire video frame does not yield satisfactory results. Temporal filtering introduces undesired errors when large motion exists, while indiscriminate spatial filtering results in blurred edges. There is a need to formulate the cause of the artifacts in greater details. We are not aware of any theoretical and systematic work that analyzes and removes rainbow-effect artifacts from the signal processing stand-point.

In this paper, we first derive the formulas governing the rainbow effects from the first principle. Based on these formulas, we propose a novel method to detect and remove the artifacts. Our detection method exploits the discriminating features in the component signals to identify the artifact regions. Two statistical features are used: (a) moments of predication errors, and (b) moments of chrominance characteristic function. Once the artifact regions are identified, we suppress the artifacts by removing large wavelet coefficients in the high-frequency subbands of chrominance component locally. Experimental results on both captured video frames and simulated frames show that our method not only remove the rainbow effect artifacts effectively, but also notably improve the image quality.

This paper is organized as follows. In section 2, we derive the formulas governing the rainbow effects. Section 3 describes the procedure for detecting the artifact region, while Section 4 provides the operations for removing the rainbow effect artifacts. Section 6 concludes the paper.

2. RAINBOW EFFECT FORMULATION

In analog composite video, primary colors *R*, *G* and *B* are first transformed into one luminance component *Y* and two chrominance components *I* and Q [4]. The *Y*, *I* and Q components are then combined into a composite signal using the following formula:

$$S = Y cos(F_y t) + I cos(F_c t) + Q sin(F_c t) \quad (1)$$

where F_y and F_c are the frequencies of the luminance and chrominance carriers, respectively.

In the receiver, the luminance *Y* and chroma $C = I cos(F_c t) + Q sin(F_c t)$ are first separated. The decoder, at times, cannot achieve a perfect separation, leaving parts of the *Y* signal in *C* signal, and vice versa. *C* remaining in *Y* causes dots crawling up the vertical edges of the image, the so-called *chroma crawl* or *dot crawl*. *Y* remaining in *C* causes rainbow-like color strips superimposed on what should be a monochromatic image, the so-called *rainbow effect*, and is the focus of this paper.

Assume that ΔY denotes the residue Y in the chroma signal, the decoded chroma signal $\widetilde{C}$ can be expressed as:

$$\widetilde{C} = \Delta Y cos(F_y t) + I cos(F_c t) + Q sin(F_c t) \tag{2}$$

To extract *I*, $\widetilde{C}$ is multiplied by $2cos(F_c t)$, which gives:

$$\begin{aligned} 2\widetilde{C}cos(F_c t) &= I + Icos(2F_c t) + Qsin(2F_c t) \\ &+ \Delta Y cos((F_y + F_c)t) \\ &+ \Delta Y cos((F_y - F_c)t) \end{aligned} \tag{3}$$

A lowpass filter is then applied to the resultant signal to remove the extra terms and recover *I*. The pass-band of the lowpass filter is usually equal to the bandwidth of the chrominance components– about 1.5 MHz. Since F_y is usually larger than 10 MHz, $F_c = F_y + 3.58MHz$ in NTSC and $F_c = F_y + 4.43MHz$ in PAL, the middle three terms can be readily removed by the lowpass filter. The last term, however, requires further analysis. In the simplest case for illustration, we assume signal ΔY contain only one frequency component ω and ΔY_0 denotes its magnitude, the last term can be expressed as:

$$\begin{aligned} \Delta Y cos((F_y - F_c)t) &= \frac{\Delta Y_0}{2} cos(\omega + (F_c - F_y))t \\ &+ \frac{\Delta Y_0}{2} cos(\omega - (F_c - F_y))t. \end{aligned} \tag{4}$$

The above expression clearly shows that if $|\omega - (F_c - F_y)|$ is smaller than the pass-band of the lowpass filter, the term $\frac{\Delta Y_0}{2} cos(\omega - (F_c - F_y))t$ will remain in the recovered *I* signal. We can therefore conclude that $2.08MHz < \omega < 5.08MHz$ and $2.93MHz < \omega < 5.93MHz$ are the luminance frequency ranges that may trigger residue rainbow effect (provided that the residue is sufficiently large) in NTSC and PAL systems, respectively.

Hence, the recovered chrominance component *I* is given by:

$$\widetilde{I} = I + \frac{\Delta Y_0}{2} cos(\omega - (F_c - F_y))t \tag{5}$$

Similarly we can obtain the recovered chrominance component *Q* as follows:

$$\widetilde{Q} = Q + \frac{\Delta Y_0}{2} sin((F_c - F_y) - \omega)t \tag{6}$$

Note that in real image signal ΔY could contain many frequency components located in the concerned frequency range, causing more than one term of interference signal.

As the erroneous terms causing chrominance artifact are sinusoidal, the rainbow effect artifacts appear as interlaced rainbow-like color stripes with frequency depending on $|\omega - (F_c - F_y)|$. We can also infer from our formulation that the strength of the artifacts is proportional to the luminance intensity. Hence, the artifacts are apparent in regions with white stripes, which possess high luminance intensity as well as high luminance frequency satisfying the above range.

Based on the above analysis, we can proceed to detect and remove the artifacts.

3. RAINBOW EFFECT DETECTION

In this section, we present a novel method to isolate rainbow-effect contaminated region, so as to avoid performing a global operation on the entire video frame, which inevitably degrades the uncontaminated area.

First, we segment the video frame into non-overlapping homogenous regions to group the contaminated pixels into an integrated region. We use Deng and Manjunath's unsupervised segmentation method [5], which is based on color quantization and spatial segmentation for region classification. The thresholds of color quantization and merging regions are set as 150 and 0.1, respectively.

The following two subsections describe the statistical features used in discriminating the artifact regions from intact region.

3.1. Moments of Prediction Errors

The primary feature used for discriminating artifact region is the *moments of prediction errors* in the luminance and chrominance components. As derived in Section 2, the rainbow effect artifacts occur in regions with high luminance frequency, and the artifacts appear as interlaced color strips, i.e., relatively high chrominance frequency. Hence, we can infer that in the artifact region, the luminance and chrominance pixel values are lowly correlated with those of their neighboring pixels. We propose to predict each pixel's value using a subset of its neighboring pixels' values and compute the moments of the error prediction.

Considering a pixel at location (x, y) having luminance value $Y(x, y)$, a linear predictor for its magnitude from the eight neighbors is given by:

$$\begin{aligned} \tilde{Y}(x, y) &= w_1 Y(x-1, y-1) + w_2 Y(x, y-1) \\ &+ w_3 Y(x+1, y-1) + w_4 Y(x, y-1) \\ &+ w_5 Y(x, y+1) + w_6 Y(x+1, y-1) \\ &+ w_7 Y(x+1, y) + w_8 Y(x+1, y+1) \end{aligned} \tag{7}$$

where w_k's are the weights. This can be expressed more compactly in a matrix form as:

$$\tilde{\mathbf{Y}} = Q\mathbf{w}, \tag{8}$$

where $\mathbf{w} = (w_1, w_2, ...w_8)^T$ is a column vector; vector $\tilde{\mathbf{Y}}$ contains the magnitudes of $\tilde{Y}(x, y)$ strung out into a column vector; and the rows of the matrix Q contain the neighboring magnitudes as specified in Eq. (7). The weights can be obtained using the Least Square Method as follow: [6]

$$\mathbf{w} = (Q^T Q)^{-1} Q^T \tilde{\mathbf{Y}}. \tag{9}$$

The error between the actual magnitude and the predicted value can be computed as

$$\mathbf{e} = |\mathbf{Y} - Q\mathbf{w}|. \tag{10}$$

The first and the second order statistics coefficients, namely, mean and variance, are obtained from the error prediction in the luminance and chrominance components, and combined into a vector of 6 coefficients. Figure 2 shows the projection of 400 intact regions and 15 artifact regions onto a 3-D linear subspace, via Principal Component Analysis (PCA). Furthermore we observe that two classes are clearly separated in 1-D space on first principle component. Thus we choose to make the classification in the first principle component projection space and set a threshold as the one maximizing Fisher discriminant [10] for classification.

Our experiments show that the detection accuracy using this feature vector is more than 95% for intact regions and 100% for artifact regions. It is, however, still likely to misclassify a few intact regions as artifact regions, especially those regions having high frequency contents in both luminance and chrominance components. To exclude these regions, we exploit another property of the artifact regions.

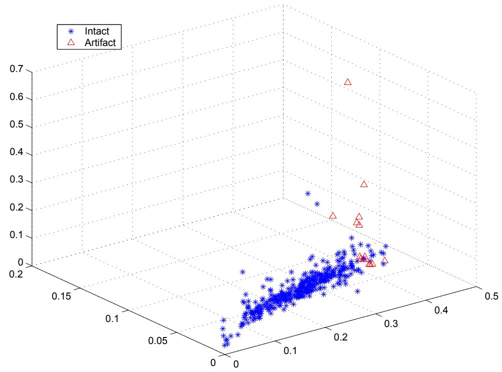

Fig. 2. Distribution of the 6-D feature vectors projected onto a 3-D subspace.

3.2. Moments of the Chrominance Characteristic Function

Equations (5) and (6) suggest that the chrominance values are symmetrical about the mean in an artifact region. Figure 3 shows an example of the chrominance histogram of an artifact region and an high-frequency intact region (misclassified using the previous feature). Moreover, the rainbow-effect artifacts are most likely to appear in regions with white stripes. Hence, the chrominance histogram of an artifact region generally has a small mean value–close to 0. On the other hand, the histogram of an intact region with high-frequency chrominance content contains more high frequency components than the artifact region.

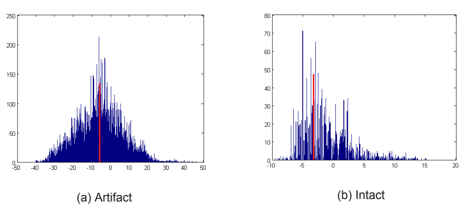

Fig. 3. Chrominance histograms of an artifact region and an intact region.

Since the normalized histogram is a probability density function (pdf), and a characteristic function (CF) can be interpreted as the Fourier transform of the pdf (with reversal in the sign of the exponent) [7], we can use the first two statistical moments of the CFs of the chrominance components as features, which are defined as follows,

$$M_n = \sum_{j=1}^{N/2} f_j^n |H(f_i)| / \sum_{j=1}^{N/2} |H(f_i)| \tag{11}$$

where $H(f)$ is the DFT of the histogram, $H(f_i)$ is the CF component at frequency f_i, N is the total number of points in the horizontal axis of the histogram.

Generally, the CF moments of artifact regions are smaller than the intact regions with high-frequency chrominance content. To take into account the characteristic of high frequencies in luminance and chrominance components, we combine the moments (M_{u1}, M_{u2}, M_{v1}, M_{v2}) with the variances as

$$s = \frac{\delta_y * \delta_u * \delta_v}{M_{u1} * M_{u2} * M_{v1} * M_{v2}} \tag{12}$$

where δ_y, δ_u, and δ_v are variances of the luminance and two chrominance components, respectively. The value s is then used to threshold the regions. Our experiments show that this additional feature is effective in excluding the misclassified intact regions.

4. RAINBOW EFFECT REMOVAL

We propose to remove the rainbow-effect artifacts in the *wavelet* domain, which is chosen for its capability of multi-resolution analysis with localization in both spatial and frequency domains [8]. Gunturk *et al.* [9] showed that high frequency wavelet coefficients of color components are strongly correlated, with correlation coefficient ranging from 0.98 to 1 for most images. As a result, the high frequency wavelet coefficients of chrominance components are generally small, and the erroneous terms causing rainbow effect artifacts usually contain large coefficients in high-frequency subbands.

Based on the symmetry property of the chrominance components and wavelet decomposition, we propose to remove the artifacts by setting the wavelet coefficients of the high-frequency subbands (LH, HL, HH) at four finest scales to their corresponding local mean value. The mean is calculated over all the pixels belonging to a homogenous region. Since the rainbow-effect artifacts degrade only the chrominance components, we process the chrominance components and leave the luminance component unchanged.

In summary, our proposed rainbow effect detection and removal algorithm consists of the following steps:

1. **Segmentation** Use Deng and Manjunath's unsupervised segmentation method [5] to segment the video frame into non-overlapping homogenous regions.
2. **Artifact Region Detection**

   (a) For each region, construct a 6-D feature vector consisting of the means and variances of the prediction errors in one luminance and two chrominance components, according to Eq. (7) to (10).

   (b) Project the feature vectors onto a 1-D linear subspace defined by the first principle component analysis (PCA) projection axis. The projection value of each region is compared against a threshold to decide the class it belongs to. The threshold is calculated to maximum the Fisher discriminant [10].

   (c) Calculate the s value according to Eq. (11) and (12) for each region identified as artifact region in (b). Set regions with $s < T_s$ or chrominance mean $m_I > T_C$ and $m_Q > T_C$ as intact regions. The thresholds $T_s = 1 \times 10^{-7}$ and $|T_C| = 10$ are determined empirically based on the training set.
3. **Artifact Removal** For the chrominance components, set the wavelet coefficients of the high-frequency subbands (LH, HL, HH) at four finest scales in the detected artifact regions to their corresponding local mean value.

5. EXPERIMENTAL RESULTS

In this section, we shall present the artifact detection and removal results of our proposed algorithm and compare with existing filtering method. The benchmark scheme used for comparison is a VirtualDub plug-in called SMIQ filter [3].

Figure 4 and Figure 5 show the results of our detection-removal method compared with the SMIQ filter on two video frames captured from composite video source. Figure 6 shows the results on a simulated frame, where rainbow effect is artificially introduced to a digital image. It can be seen that our algorithm works well for the captured video frames as well as the simulated frame. The restored frames have significant visual quality improvements compared with the degraded ones as well as the results obtained using the SMIQ filter. For the simulated frame, the Peak Signal-to-Noise Ratio (PSNR) of the R, G, and B components of the restored frame are 33.38 dB, 38.28 dB, 31.08 dB, respectively, using our proposed method. There is a clear improvement from 33.08 dB, 37.32 dB, and 29.69 dB before restoration.

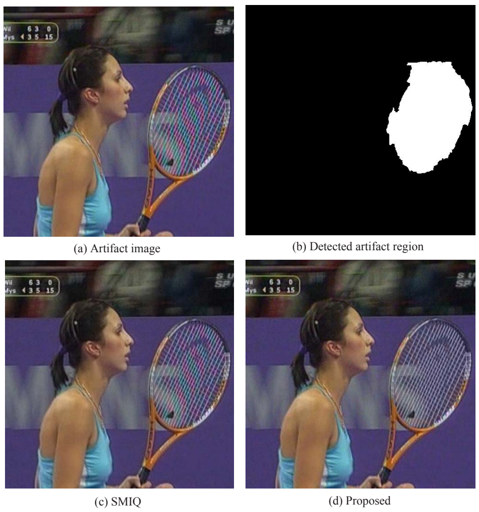

Fig. 4. Results on captured video frame I: (a) the artifact frame, (b) the detected artifact region, and restored frames using (c) SMIQ filter, (d) our proposed method.

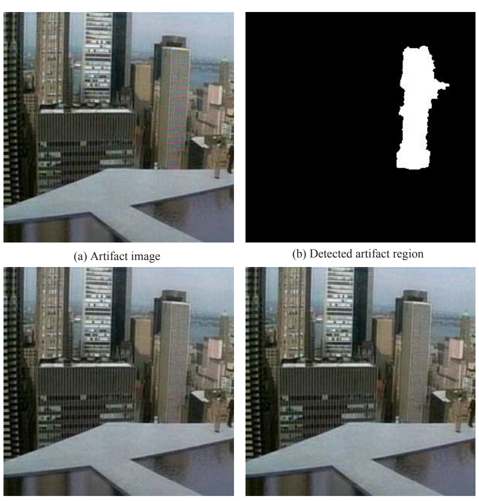

Fig. 5. Results on captured video frame II: (a) the artifact frame, (b) the detected artifact region, and restored frames using (c) SMIQ filter, (d) our proposed method.

6. CONCLUSION

In this paper, we derive the formulas governing the rainbow-effect artifacts from the first principle. Based on these formulas, we propose a novel method to detect and remove these artifacts. Our detection method exploits the features in the luminance and chrominance components to discriminate the artifact regions. Two statistical features are used: (a) moments of prediction errors, and (b) moments of chrominance characteristic function. Once the artifact regions are identified, we suppress the artifacts by modifying large wavelet coefficients in the high-frequency subbands at these detected regions. Experiments conducted on both captured video frames and simulated frames demonstrate our method not only removes the rainbow effect artifacts effectively, but also notably improves the visual quality.

Fig. 6. Results on a simulated video frame: (a) the simulated artifact frame, (b) the detected artifact region, restored frames using (c) SMIQ filter, and (d) our proposed method.

7. REFERENCES

[1] J. F. Blinn, “Ntsc: nice technology, super color,” *IEEE Computer Graphics & Applications*, vol. 13, no. 2, pp. 17–23, March 1993.

[2] Wilbert, “Removing rainbow effects and dot crawls,” *http://big5.doom9.org/capture/rainbows.htm*.

[3] *http://www.doki.ca/filters/*.

[4] A. M. Tekalp, *Digital Video Processing*. Prentice Hall PTR, Prentice - Hall. Inc., 1995.

[5] Y. Deng and B. S. Manjunath, “Unsupervised segmentation of color - texture regions in images and video,” *IEEE Trans. on Pattern Analysis and Machine Intelligence*, vol. 23, no. 8, Aug. 2001.

[6] B. Windrow and S. Stearns, *Adaptive Signal Processing*. New Jersey, Prentice Hall, 1990.

[7] A. Leon-Garcia, *Probability and Random Processes for Electrical Engineering*. 2nd Edition, Reading, MA: Addison-Wesley Publishing Company, 1994.

[8] M. Malfait and D. Roose, “Wavelet-based image denoising using a markov random field a prior model,” *IEEE Trans. on Signal Processing*, vol. 6, no. 4, pp. 549–565, Apr. 1997.

[9] B. K. Gunturk, Y. Altunbasak, and R. M. Mersereau, “Color plane interpolation using alternating projections,” *IEEE Transcations on Image Processing*, vol. 11, no. 9, 2002.

[10] R. Fisher, *The Use of Multiple Measure in Taxonomic Problems*. Annals of Eugenics, 1936.